Supporting Information

Three-dimensional organization of self-encapsulating *Gluconobacter oxydans* bacterial cells

Vi Khanh Truong,[†] Chris M. Bhadra,[†] Andrew J. Christofferson,[‡] Irene Yarovsky,[‡] Mohammad Al Kobaisi,[†] Christopher J. Garvey,[|] Olga N. Ponamoreva,[l] Sergey V. Alferov,[l] Valery A. Alferov,[ll] Palalle G. Tharushi Perera,[†] Duy H. K. Nguyen,[a] Ričardas Buividas,[†] Saulius Juodkazis,[†] Russell J. Crawford,[‡‡] Elena P. Ivanova[†*]

[†]School of Science, Faculty of Science, Engineering and Technology, Swinburne University of Technology, Hawthorn VIC 3122, Australia

[‡]School of Engineering, RMIT University, GPO Box 2476, Melbourne 3001, Australia

[|]Australian Nuclear Science and Technology Organisation, Locked Bag 2001, Kirrawee DC NSW 2232.

[l]Biotechnology Department and [ll]Chemistry Department, Tula State University, 92 Lenin pr. Tula 300012 Russian Federation

[‡‡]School of Science, RMIT University, Melbourne VIC 3001, Australia

*Corresponding Author

Prof. Elena Ivanova

Email: eivanova@swin.edu.au

Keywords. Hydrogels, self-encapsulation, three-dimensional organization, bacterial extracellular polysaccharide, *Gluconobacter oxydans*

Movie S1. Self-assembly of *G. oxydans* in PVA-VP system over a one hour period.

Movie S2. Time-lapsed CLSM showing the self-assembly of *G. oxydans* in PVA-VP over a 24 hour period.

Movie S3. Interactions between acetan and PVA-VP polymer.

S1. Supporting materials and methods

S1.1. Swelling ratio analysis

The rate of water uptake of PVA-VP hydrogels was evaluated using the swelling ratio. For calculation purposes, the dry weight of the films was recorded before the start of the experiment. An average value was obtained after 4 independent runs. The equilibrium swelling ratio was calculated as given by Equation (1):

$$Swelling\ ratio\ (\%) = \frac{W_s - W_d}{W_d} \times 100 \qquad (1)$$

Here, W_s denotes the weight of swollen film while W_d denotes the weight of dry film. The hydrogel samples were swollen in Milli-Q water for 30, 60, 90 and 120 minutes (2 h) respectively at 25 °C. The dry weights of the films were recorded at the beginning of the experiment. It was observed that that an equilibrium swelling value was obtained after a time period of 120 minutes. After the stipulated time-period, the hydrogels were wiped using a soft tissue paper to remove the excess water and the readings were recorded immediately.

S1.2. Synthesis of PVA-VP and nanoparticle-immobilized PVA-VP

An aqueous PVA solution (5 wt. %) was prepared by dissolving PVA in MilliQ water at 80 °C under constant magnetic stirring. The solution was subsequently cooled to room temperature. A 0.1 mL volume of N-vinyl pyrrolidone (VP) monomer was added into the PVA solution under magnetic stirring at a temperature maintained at 40 °C. Ceric ammonium nitrate (CAN) was added as an initiator (0.8 mL) of the free-radical polymerization reaction. The entire system was purged continuously with N_2 for three hours to remove any oxygen present. The resulting homogenous polymer solutions were cast on a glass side (76 mm × 26 mm × 1 mm) for further characterization. An aqueous solution of ammonium cerium (IV)

nitrate $(NH_4)_2Ce(NO_3)_6$ (0.8 mL, T = 0.1 g/mL) and N-vinyl pyrrolidone (0.1 mL) were added to aqueous solutions of PVA (20 mL, 5% w/v) with stirring at 40 °C. Nitrogen gas was passed through the solutions for 3 h to remove any dissolved oxygen. The resultant hydrogel was used as a matrix for the encapsulation of the microorganisms.

The method of synthesizing fluorescent dye-encapsulated silica NPs was adopted from a previous study [1, 2]. Ruthenium-tris(4,7-diphenyl-1,10-phenanthroline) dichloride (Ru(dpp)) solution (5 mL) was prepared in dichloromethane at a concentration of 1 mg/mL before mixing with 1 g Pluronic® F-127. Typically, after the surfactant completely dissolved, the solution was evaporated under a flow of nitrogen at room temperature (*ca.* 22 °C). When the mixture was completely dry, hydrochloric acid (0.85 M, 15.6 mL) was added and stirred until a homogeneous solution was obtained. TEOS (1.8 mL) was then added to the homogeneous solution; and the hydrolysis of TEOS was allowed to take place for 105 minutes. Finally, the silica-particle growth was terminated by the dropwise addition of DMDMS (150 µL) under constant stirring for 24 h at room temperature. The unreacted and excess chemicals were removed by dialysis over 7 days using a molecular weight cutoff at 14000 Da with excess of MilliQ water. The final suspension was filtered through a 0.2 µm Teflon filter in order to collect a uniform particle suspension without any large aggregates. A solution of the fluorescent nanoparticles (1 mL) was added to the cross-linked PVA hydrogel (2 mL) and stirred for 15 minutes.

S1.3. Microbial fuel set-up

The biofuel cell consisted of two connected chambers as previously published [3] (Figure S1). The working volumes of the anode and a cathode compartments were the same (3 mL). Spectrographic graphite rods with a diameter of 8 mm and a work surface of 300 mm^2 were used as electrodes (SEU; Research Institute of Electrocarbon Products, Russia). Prior to bacterial immobilization, graphite rods were immersed with 50 mL of nitric acid (density of 1.35 g/mL) at 78 – 80 ºC for 15 min. Mixture of 200 µL PVA-VP and 30 mg of *G. oxydans* were spread along the graphite electrode. For suspended cells, only 30 mg of *G. oxydans* were spread on graphite. Both of immobilizations were applied to obtain the cell density of 0.1 mg/mm^2.

Electrodes were immersed in a solution for 10 mm. The anode and cathode compartments were separated by a Nafion 117 membrane with a diameter of 6 mm. 30 mM sodium

phosphate buffer, pH 6.0, was used as a background solution. For estimation of the catalytic efficiency of *G. oxydans*, 3 mM potassium ferricyanide (III) was used in the cathode compartment, together with 0.08 mM 2,6-dichlorophenolindophenol (2,6-DCPIP) in the anode compartment. All of the reagents were of analytical grade. IPC Micro potentiostat (Volta, Russia) was used to measure the resistance between cathode and anode. The internal resistance was calculated by measuring the voltage (potential) to the external resistance, at the maximum power (translation needs editing). The maximum MFC voltage is reached when external and internal resistances are equal[4]. The internal resistance was calculated by measuring the voltage (potential) on the external resistance, at the maximum power generation according to the equation:

$$R_{\text{int}} = \frac{E_{emf} - E_{\max}}{I_{\max}}$$

where E_{emf} is the generated potential when external circuit is unlocked, $I_{\max}$ and $E_{\max}$ is current and voltage measured at the external resistance at maximum power output.

And maximum power output was calculated according to the equation:

$$P_{an} = \frac{E_{\max}^2}{A_{an} R_{ext}}$$

where A_{an} is the anode surface square, R_{ext} is an external resistance, $E_{\max}$ is voltage measured at the external resistance.

S2. Supporting Results and Discussion

S2.1. Performance analysis of the constructed microbial fuel cell (MFC)

Working towards improving the overall efficiency of a microbial fuel cell, the microbial fuel cell (MFC) performance analysis using *G. oxydans*-integrated hydrogel as the bio-anode is shown in Table S1 and Figure S4. A maximum generated voltage of 48.0 and 90.0 mV/mg was obtained for suspended and respectively (Table S1). Encapsulated *G. oxydans* requires only 20-30 mins to generate 90.0 mV/mg of bacteria while suspended bacteria can only produce 48.0 mV/mg after 60-70 mins. In particular, resistance of encapsulated *G. oxydans* is three-time lower than suspended bacteria, i.e. electron conductivity of encapsulated *G.*

oxydans is much higher than suspended bacteria. After 18-hour incubation, the generated potential decreases as the suspended bacteria undergo a transition from stationary growth phase towards the beginning of decline phase. However, the generated potential of encapsulated *G. oxydans* remains to be stable with the voltage of 90 mV/mg during eight day-operation (Fig. S4B).

Cyclic voltammogram (CV) have been made in three electrode (counter - Ag/AgCl, reference - Pt, working - graphite) electrochemical cell, using potentiostat Ecotest-VA (Econiks-Ekspert, Russia) in the range of potential from -600 to 600 mV, and scanning rate of 25 mV/s. To investigate the effect of bacterial clusters, cyclic voltammograms were recorded for bare graphite electrode with free-suspended bacteria at the electrochemical cell (Fig. 4A and B) and PVA-VP/*G. oxydans*- modified electrode (Fig. 4C and D). There is a significant difference of CVs. The $E^{0'}$ of PVA-VP/*G. oxydans*- modified electrode with 2,6-DCPIP and glucose is 1.10 V. However, the $E^{0'}$ of bare graphite electrode with free-suspended bacteria is 0.55 V. The average time of signal generation significantly increased with an increasing amount of a biocatalyst and varied within a range of 30 – 130 min. Bioanodes with the surface density of immobilized cells of approximately 3–10 mg/cm^2 should be used in order to obtain the maximum MFC voltage and to decrease the time of reaching the stationary value.

S2. Supporting Tables and Figures

Table S1. Power production characteristics of *G. oxydans* at the suspended and PVA-VP encapsulated states.

Type of biocatalyst	Generated potential, mV/mg of bacterial cells	Time for maximum potential generation, min	Internal resistance, kΩ	Resistivity, kΩ.m	Conductivity, mS/m	Power density mV/m^2
Suspended bacterial cells	48	60-70	300	9.42	0.11	0.07
Encapsulated bacterial cells	90	25-30	100	3.14	0.32	2

Table S2. Properties of the polysaccharide/PVA-VP systems inferred from molecular dynamics studies.

Polysaccharide	Molecular weight (g/mol)	Density Difference[a] (atoms/Å^3)	Radius of Gyration (Å)	% contact[b]	H-bonds to PVA-VP (population)
acetan ($C_{46}H_{73}O_{38}$)	1234	0.06	7.4 ± 1.4	45 ± 1%	8 ± 3%
cellulose ($C_{42}H_{72}O_{36}$)	1153	0.03	10.6 ± 0.3	40 ± 1%	7 ± 3%
dextran ($C_{42}H_{72}O_{36}$)	1153	0.03	6.4 ± 0.6	34 ± 1%	6 ± 2%
levan ($C_{42}H_{72}O_{36}$)	1153	0.02	6.6 ± 0.5	41 ± 2%	7 ± 4%

[a] Absolute value of the difference in PVA-VP atomic density with and without the presence of the polysaccharide
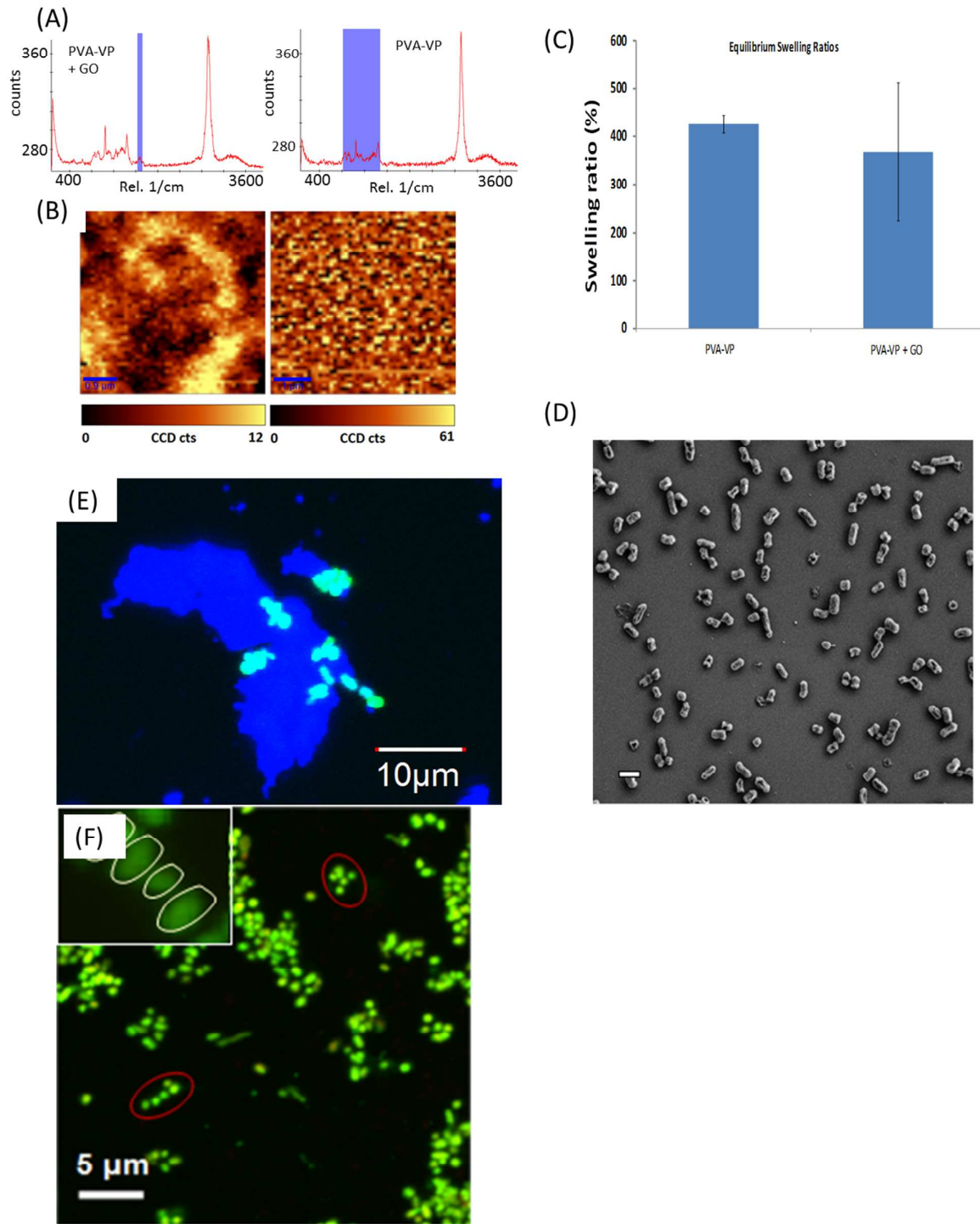[b] Percentage of polysaccharide solvent-accessible surface area in contact with PVA-VP

Figure S1. (A) Raman spectra (at 532 nm laser) of encapsulated *G. oxydans* and hydrogel. Raman imaging using 1600 to 1720 cm^{-1} Raman shift range with the intensity profile map of the same images of corresponding samples. (B) Swelling ratios of the PVA-VP hydrogels and their *G. oxydans* (GO) encapsulated counterparts. (C) The readings are taken at time duration of 120 min (2 h) and the error bars represent the deviation from 4 independent measurements.

(D) Morphology of *G. oxydans* cells visualized by scanning electron microscopy (SEM) (scale bar 2 μm). (E) Confocal laser scanning microscopy (CLSM) image showing the exopolysaccharide (EP) covering around *G. oxydans* cells (EPS stained with Alexa 633 Concanavalin A (blue color) and viable cell stained with SYTO$^{®}$ 9 (green color)). (F) CLSM showing the side by side alignment of the *G. oxydans* cells in the PVA-VP.
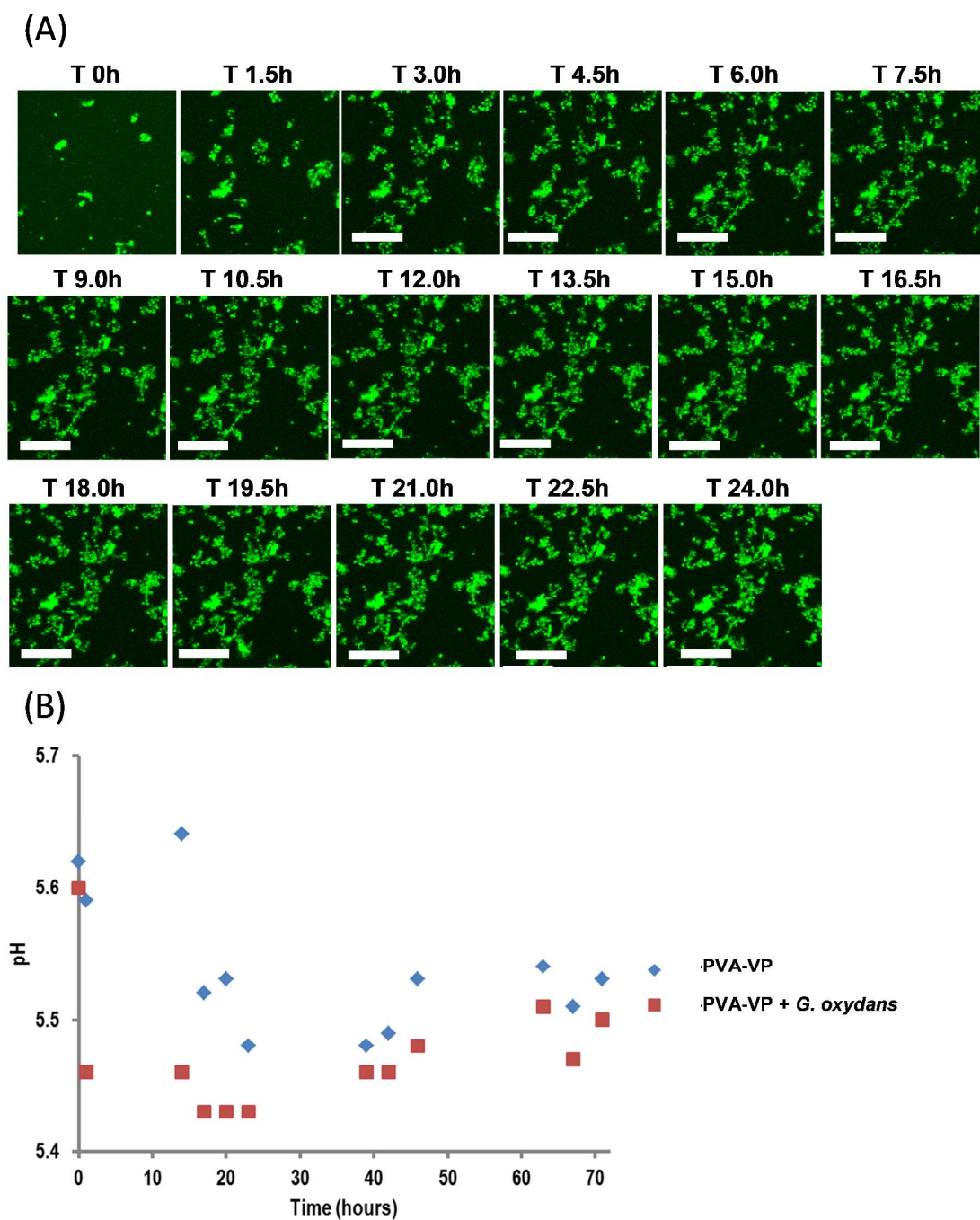
(A)

(B)

Figure S2. (A) Time-lapsed self-assembly of *G. oxydans* in PVA-VP over 24 hours. (B) Dynamic pH changes of PVA-VP and PVA-VP + *G. oxydans*.
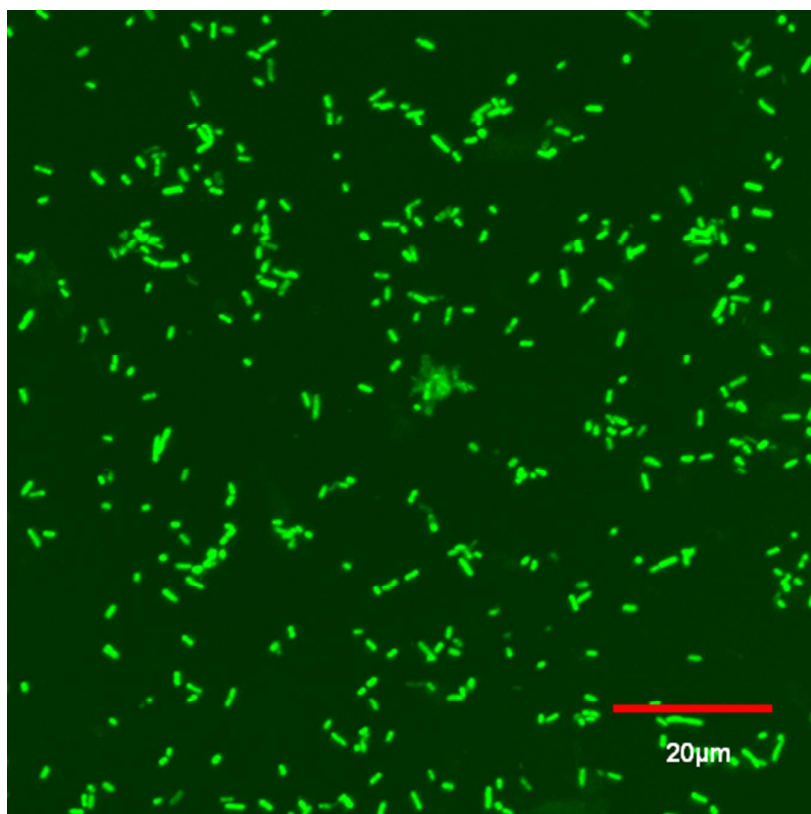
Figure S3. *Escherichia coli* cells with the PVA-VP hydrogels. CLSM images showing lack of any self-organization.
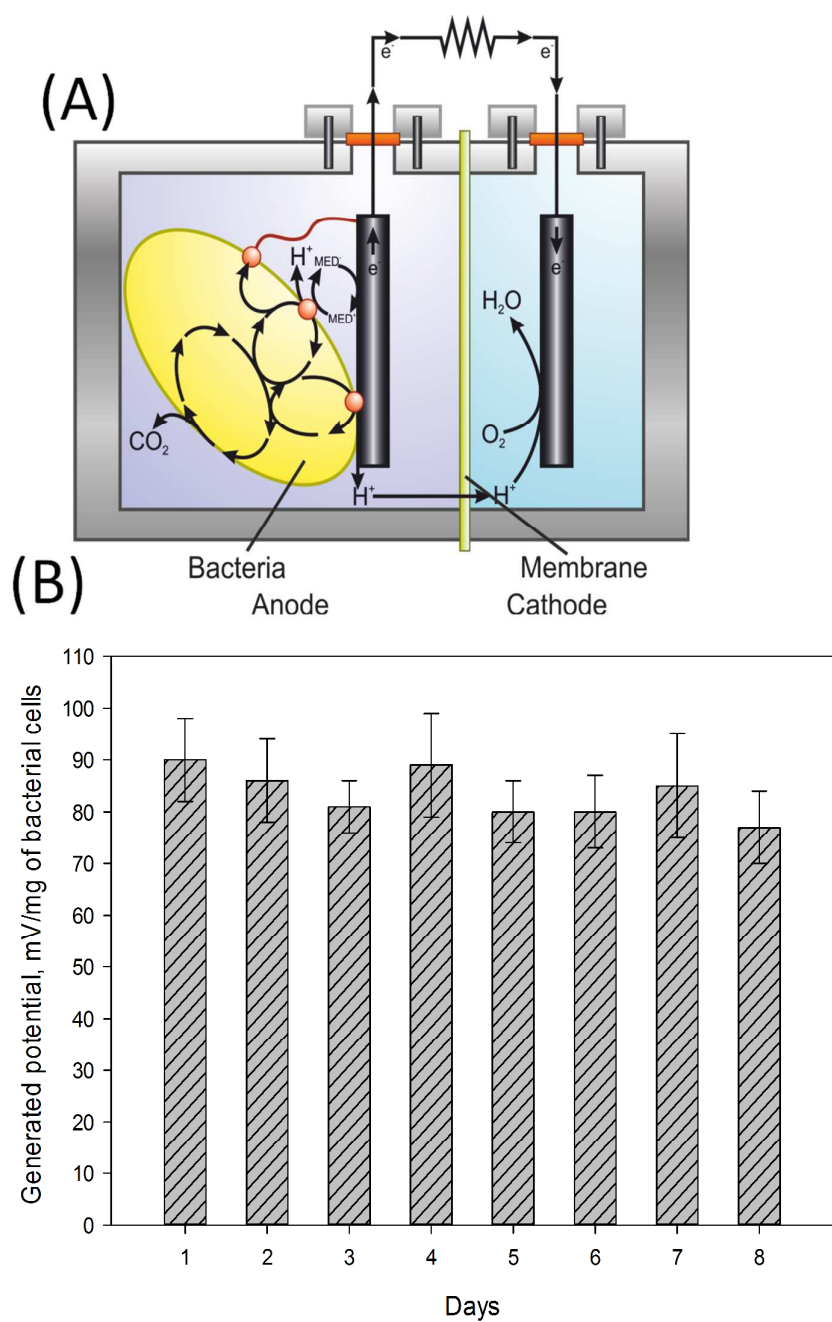
Figure S4. Microbial fuel cell (MFC) performance analysis. (A) Schematic of microbial fuel cell set-up, and (B) The long-term stability of encapsulated *G. oxydans* showing the electricity generation.

References

1.   Wang, X.-d.; Stolwijk, J. A.; Lang, T.; Sperber, M.; Meier, R. J.; Wegener, J.; Wolfbeis, O. S. Ultra-small, highly stable, and sensitive dual nanosensors for imaging intracellular oxygen and pH in cytosol. *J. Am. Chem. Soc.* **2012**, *134*, 17011-17014.
2.   Truong, V. K.; Mainwaring, D. E.; Murugaraj, P.; Nguyen, D. H. K.; Ivanova, E. P. Impact of confining 3-D polymer networks on dynamics of bacterial ingress and self-organisation. *J. Mater. Chem. B* **2015**, *3*, 8704-8710.
3.   Alferov, S. V.; Minaicheva, P. R.; Arlyapov, V. A.; Asulyan, L. D.; Alferov, V. A.; Ponamoreva, O. N.; Reshetilov, A. N. Bioanode for a microbial fuel cell based on *Gluconobacter oxydans* immobilized into a polymer matrix. *Appl. Biochem. Microbiol.* **2014**, *50*, 637-643.
4.   Logan, B. E. *Microbial fuel cells*. John Willey and Sons: New York, 2008; p 216.